High Power Diamond Raman Lasers

Robert J. Williams, Ondrej Kitzler, Zhenxu Bai, Soumya Sarang, Hadiya Jasbeer, Aaron McKay, Sergei Antipov, Alexander Sabella, Oliver Lux, David J. Spence, and Richard P. Mildren

(Invited Paper)

***Abstract*—Laser gain materials possessing high thermal conductivity and robust mechanical properties are key prerequisites for high power lasers. We show that diamond, when configured as a Raman laser, enables access to these and other extreme properties, providing an important new route to high power and high brightness beam generation. Recent achievements in pulsed and continuous wave oscillators, beam combining amplifiers, and single longitudinal mode oscillators are summarized, along with wavelength extension of these concepts through adaption to other pumps, use of Raman cascading, and intracavity harmonic generation. To date, diamond laser powers have attained 750 W with efficiency and beam quality so far unperturbed by nonlinear or thermally induced side-effects. Large factor brightness enhancement of low coherence inputs is demonstrated using multiple pump beams (via Raman beam combination) or highly multimode pumps for oscillator and amplifier configurations. Future directions for direct diode pumping, and for realizing extraordinary power and power density through reduced temperature operation and isotopically enriched diamond, are also discussed. Our results indicate that diamond is emerging as a generic high-power laser technology with advantages in terms of brightness (high average power and high beam quality) and wavelength range.**

***Index Terms*—Diamond, lasers, laser beams, optical materials, power lasers, power amplifiers, Raman scattering.**

I. Introduction

DIAMOND has a distinguished position amongst materials as the element of lowest atomic number to form a covalently bonded lattice. Extreme hardness, high thermal conductivity and chemical inertness are the consequence, as well as an array of other lesser-known outstanding properties. In optics, diamond was originally sought after as a high index material for high magnification microscopes [1] or as an infrared transmitting window for extreme environments [2], [3]. Just like other precious gemstones such as ruby, garnets and sapphire, its robust mechanical properties, high thermal conductivity and wide transmission range are immediately attractive as a host for fluorescent laser ions [4]. Unfortunately, however, these ambitions have gone largely unfulfilled because of the difficulties involved in introducing suitable dopants into the dense lattice structure without compromising its core material advantages [5], [6]. On the other hand, its high atomic density and strong bonding, in combination with a highly symmetric lattice, lead to a high Raman gain coefficient and hence an alternative means for light amplification. The material advantages of undoped diamond are thus available to benefit laser technology, albeit with all the particularities of a Raman laser medium.

Although the Raman laser concept is now over 50 years old, interest in diamond as a Raman laser material has only intensified in the last decade with the availability of high quality synthetic crystals. Prior to 2008, there had been only a handful of reported demonstrations showing Raman gain. Stimulated Raman scattering (SRS) was observed as early as 1963 by Eckhardt *et al.* using a Q-switched ruby laser pump as part of a study involving a survey of several promising materials [7]. Even at this early stage, both diamond and its Group IV sibling silicon were recognized as good candidates for high gain Raman lasers [8]. In 1970, McQuillan *et al.* reported a reduction in threshold using the 17% Fresnel reflections of the uncoated surfaces [9]. In these early demonstrations involving "giant pulse" pumping from a ruby laser, the output also included anti-Stokes lines and higher-order cascaded lines. Levenson *et al.* [10], [11] later used diamond as a sample for investigating dispersion and interference of the Raman and electronic nonlinearities.

The first report of Raman laser phenomena using synthetic diamond was in 2003 with measurements of SRS spectra using a sample grown by chemical vapor deposition (CVD) in the USA [12]. In the subsequent few years (2003–8), CVD-grown material from Russia and the UK led to several reports of SRS [13], [14] and a Raman laser with external mirrors [15]. At this time, the development of Raman lasers based on crystals such as barium nitrate, and those in the tungstate and vanadate classes, had attained a mature stage [16]. Diamond was quickly incorporated into a variety of Raman laser formats including intracavity pumping in pulsed [17] and continuous wave (CW) formats [18], and synchronous pumping for picosecond pulsed output

Manuscript received December 11, 2017; revised March 29, 2018; accepted April 2, 2018. Date of publication April 16, 2018; date of current version May 18, 2018. This work was supported in part by Australian Research Council (ARC) under Grant DP150102054 and Grant LP160101039, in part by U.S. Air Force Research Laboratory (FA2386-15-1-4075), and in part by U.S. Army International Technology Center Pacific ITC-PAC (FA5209-15-P-0170). *(Corresponding author: Richard P. Mildren.)*

R. J. Williams, O. Kitzler, Z. Bai, S. Sarang, H. Jasbeer, A. McKay, S. Antipov, D. J. Spence, and R. P. Mildren are with the MQ Photonics Research Centre, Macquarie University, Sydney, NSW 2109, Australia (e-mail: rich.mildren@mq.edu.au).

A. Sabella is with the Cyber and Electronic Warfare Division, Defence Technology Group, Edinburgh, SA 5111, Australia.

O. Lux is with the Institut für Physik der Atmosphäre, Deutsches Zentrum für Luft- und Raumfahrt, Oberpfaffenhofen, Weßling 82234, Germany.

Color versions of one or more of the figures in this paper are available online at http://ieeexplore.ieee.org.

Digital Object Identifier 10.1109/JSTQE.2018.2827658

[19]. The material quality and high gain properties enabled high laser efficiencies to be achieved [20]–[22] compared to other Raman crystals (despite having a relatively large quantum defect as discussed in Section II-A). As a consequence of its large transmission range, diamond Raman lasers (DRLs) have been demonstrated at wavelengths as short as 273 nm [23] and as long as 3800 nm in first Stokes [24] and 7300 nm in second Stokes order [25]. Recent advances in fabrication of low-loss waveguides have led to the demonstration of on-chip DRLs [26], [27]. Thus the confluence of high quality diamond synthesis with Raman laser technology has led to rapid development of a diverse range of novel laser devices.

By far and away the most outstanding property of diamond is its thermal conductivity, being approximately 150 times higher than YAG and 60 times higher than sapphire (at room temperature), laser hosts that are ubiquitous in large part due to their high thermal conductivities. The thermal conductivity parameter is explicit in most mechanisms responsible for laser power limits and it is this diamond advantage that forms a primary motivation for our research. This paper briefly reviews the progress in high power diamond lasers and reports our latest achievements in devices operating across a range of temporal, spatial and spectral regimes. New and updated results are presented in most of these directions of research. For previously published work, each instance is cited to indicate the location of further details. As introduction, the distinctive properties of the Raman laser gain mechanism and the material parameters central to performance are summarized (Section II). We then describe our research in the areas of high power oscillators (Section III), brightness enhancement in CW lasers and pulsed amplifiers and lasers (Section IV), intracavity frequency-doubled lasers (Section V) and single longitudinal mode (SLM) lasers (Section VI). The article concludes with a discussion of opportunities for future development and applications (Section VII).

II. Characteristics of Raman Gain in Diamond

Raman lasers and diamond both have their own long histories, mostly separate from each other. This Section provides brief summaries of the basic properties of crystalline Raman lasers (described through the prism of familiar inversion laser concepts) and the properties of diamond that are critical to DRL design and capability.

A. Raman Versus Inversion Lasers

Optically-pumped lasers are essentially devices that alter the wavelength and spatio-temporal properties of input light using the principle of optical amplification. Raman lasers and optically-pumped inversion lasers fall into this category but are distinguished by their respective amplifying mechanisms. The amplification in inversion lasers has gain proportional to the stimulated emission cross-section and the inversion density created by absorption of optical input (pump) power. The immediate energy source for the laser field is the stored pump energy in the population inversion. In Raman lasers, gain (in steady-state) is proportional to the product of the pump intensity I_P and the material parameter called the Raman gain coefficient g_R. The proximate energy source in this case is the pump field itself. The output wavelength is the Stokes-shifted wavelength ($\lambda_s = (1/\lambda_p - \upsilon_R/c)^{-1}$ where ν_{R} is the frequency in Hz of the Raman vibration) in contrast to the fixed output spectrum of an inversion laser according to the energy level structure of the fluorescent lasant species.

The contrasting Raman gain mechanism brings forth a range of distinctive properties that influence laser design and capability. The detailed theory and properties of Raman gain media have been described many times previously (eg., [28]–[32]). The following aims to provide a brief and qualitative summary of the main features of Raman gain responsible for the broader range of phenomena observed.

1) Large Output Wavelength Choice: In principle, Raman media can generate gain across their whole transmission band according to the selected pump laser wavelength. It follows from the free choice of pump wavelength that the process can be cascaded to second- or higher-order Stokes fields to generate wavelengths much further spaced from the pump. Broadly tunable output may be achieved via tuning the pump laser wavelength. Tuning range may also be derived from the Raman linewidth, however, in crystals this is typically less than 200 GHz.

2) No Energy Storage in the Material: Because Raman gain depends directly on the pump field intensity, gain persists for only as long as the pumping duration (in contrast to inversion lasers where gain lasts for the life of the inverted population). Hence, Raman lasers may be referred to as 'gain-switched' with output pulses of similar or shorter duration than the pump (with significant pulse compression possible with backward amplifiers [33] and ultrafast Raman oscillators [34]). The lack of energy storage in a stimulated scattering medium dictates that there is no direct analog for Q-switching in Raman lasers.

3) Require Bright Pump Sources: For inversion lasers, the capacity to accumulate and store pump energy permits practical gain values using low brightness optical pumps. For Raman crystals, with g_R values of the order of 10 cm/GW, the intensities required to reach threshold are typically well above tens of MW/cm^2. As a result, picosecond- and nanosecond-pumped Raman lasers were the first developed. CW devices have only been developed in the last two decades with the use of high finesse cavities and high gain materials [35], [36].

4) Require Narrow Linewidth Pumps: Whereas inversion lasers are generally accepting of broad pump sources according to the absorption bands of the material, the Raman gain mechanism relies on the coherent generation of a phonon field in the medium thus imposing more stringent requirements on the pump spectrum. Under all but some circumstances (see refs [37]–[39] for detail), pump bandwidths larger than the Raman linewidth (45 GHz for diamond) lead to an approximately proportional reduction in gain [37].

5) No Spatial Hole Burning: The energy depleted preferentially from anti-node regions of a standing-wave cavity mode in inversion lasers is referred to as spatial hole burning (SHB). As a further consequence of the lack of energy storage in the stimulated scattering medium, there is no simple equivalent to SHB in Raman lasers [40]. Raman lasers thus avoid common

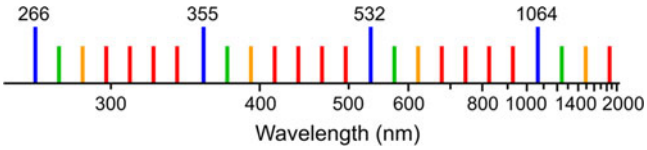

Fig. 1. The wavelengths accessible from diamond by cascaded-Stokes lasing from fundamental and harmonics of 1.06 μm (blue lines). The first and second Stokes wavelengths are indicated by green and orange lines, respectively.

side-effects of SHB such as longitudinal-mode instabilities [41] and potentially also high intensity noise in intracavity frequency doubled configurations (the 'green problem' [42]).

6) Automatically Phase-Matched: In most cases, Raman gain is independent of the input beam direction with respect to the output beam. This feature, a consequence of the freedom for phonons to take any *k*-vector owing to their flat dispersion relation [31], is the critical aspect that makes Raman lasers share many properties of inversion lasers and sets them apart from nonlinear wave mixing processes such as $\chi^{(2)}$ parametric oscillators. This enables generation of high brightness output from low-beam-quality inputs [43], [44] and multiple non-collinear pumps (Raman beam combination) [45] as well as offering potential for side-pumped configurations [46].

B. Diamond Material Properties

As with any laser material, the properties determining diamond's suitability are numerous and varied. The most central of these to Raman laser performance are Raman frequency spectrum, transmission range, gain coefficient and thermal conductivity. The Raman spectrum contains a single triply-degenerate Raman mode with a room-temperature frequency of 39.969 THz (1332.3 cm^{-1}) and full width at half-maximum of 45 GHz. The Raman frequency is highest among the recognized Raman crystals, which typically fall in the range 10–30 THz. By cascading, the wavelength gaps between laser harmonics are accessible as indicated in Fig. 1 for the example of a Nd:YAG pump laser. With first-order lattice absorption forbidden, diamond possesses a very wide transparency range from the bandgap wavelength at 225 nm to beyond the far-infrared, with the exception of a multi-phonon absorption region between 2.5–6 μm (see Fig. 2).

The Raman gain coefficient is dependent on wavelength as indicated by experimental and theoretical data in Fig. 2. Although there is a considerable spread in measured values, there is broad agreement with the semi-empirical theoretical predictions of [47]. For input and output polarizations parallel to the $\langle 111 \rangle$ crystallographic direction, the coefficient is approximately 10 cm/GW at a pump wavelength of 1 μm. It scales proportionally with Stokes frequency, apart from an enhancement on approach to the bandgap where values above 100 cm/GW are obtained. Diamond has a high gain coefficient compared to other Raman crystals with some notable exceptions; barium nitrate in the visible (47 cm/GW at 532 nm [48]) and silicon between 1 and 2 μm (20 cm/GW at 1550 nm [49]).

The material properties most relevant to high power generation are the thermal expansion coefficient α_T, thermo-optic coefficient $\mathrm{d}n/\mathrm{d}T$, laser-induced damage threshold (LIDT) and

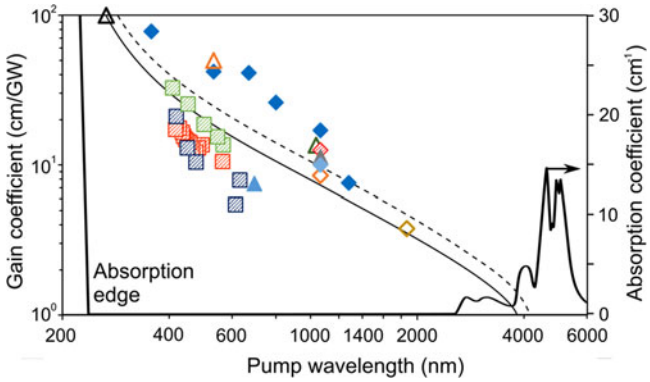

Fig. 2. Wavelength dependence of g_R obtained using the following methods: pump probe (diamonds) [38], [45], [50]–[52]; SRS threshold (triangles) [9], [14], [23], [53]; spontaneous Raman scattering (squares) [11], [47]. Pump polarization parallel to: $\langle 111 \rangle$ (full symbols); $\langle 110 \rangle$ (open symbols); $\langle 100 \rangle$ (hatched symbols). The thin solid and dashed lines are calculated gain coefficients [47] for a linear pump polarization parallel to $\langle 110 \rangle$ and $\langle 111 \rangle$, respectively. Figure adapted from [38]. A room temperature absorption spectrum of optical grade CVD diamond is also shown (thick solid line) [54].

TABLE I
THERMAL AND NONLINEAR EFFECTS IN END-PUMPED LASERS: COMPARISON OF DIAMOND WITH ND:YAG

Effect	Functional Dependence	Nd:YAG: diamond[a]
End-face bulging strength [56]	$\alpha_\mathrm{T}\,(n\text{-}1)(\nu\text{+}1)/\kappa$	919:1
Radial stress-induced birefringence strength [55]	$\alpha_\mathrm{T}\,n^3\,C_r/\kappa$	739:1
Thermo-optic lens strength [55]	$\mathrm{d}n/\mathrm{d}T\,/\kappa$	88:1
Kerr lens strength [57] [b]	n_2	1.5:1
Bulk stress fracture threshold [58]	$\kappa(1\text{-}\nu)/(\alpha_\mathrm{T}\,E)$	1:456
CW coating damage threshold [59]	κ	1:182

[a] evaluated at room temperature assuming an end-pumped circular rod.
[b] at 1 μm
n – refractive index, n_2 – nonlinear refractive index, ν – Poisson ratio, C_r – a parameter containing radial elasto-optical coefficients, E – Young's modulus.

thermal conductivity κ. In order to provide an indication of the power-scaling capacity of diamond over other laser materials, we have compared the strength of thermally-induced effects with end-pumped Nd:YAG (material parameters from [55]), a high power laser crystal that is also isotropic. As shown in Table I, the combination of a low thermal expansion coefficient ($1.1 \times 10^{-6}\ \mathrm{K}^{-1}$) and exceptionally-high thermal conductivity (2000 W/m·K) yields two to three orders-of-magnitude improvements in terms of shape distortion, stress birefringence and the threshold for bulk stress fracture [54]. The thermo-optic coefficient of diamond ($1.5 \times 10^{-5}\ \mathrm{K}^{-1}$) is approximately twice as high as YAG, but the much higher thermal conductivity leads to an overall large reduction in the thermo-optic lens strength.

Cooling laser crystals to cryogenic temperatures is widely used for increasing power range as the thermo-mechanical and thermo-optical material properties are often improved substantially. In diamond of natural isotopic composition (1.1% ^{13}C), the thermal expansion and thermo-optic coefficients decrease

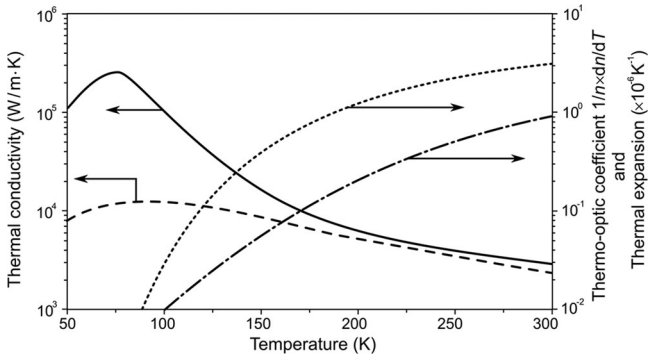

Fig. 3. The thermal conductivity of natural (1.1% ^{13}C; dashed line) [60] and enriched diamond (0.001% ^{13}C; solid line) [61], the thermo-optic coefficient $1/n \cdot \mathrm{d}n/\mathrm{d}T$ (dotted line [54]) and thermal expansion coefficient (dash-dotted [62]) for natural IIa diamond as a function of temperature.

by orders of magnitude, and the thermal conductivity increases by a factor of five at 78 K compared to room temperature (as shown in Fig. 3). However, it should be noted that in the case of pulse durations shorter than the thermal diffusion time (120 ns for a pump radius of 160 μm at 78 K) the temperature rise is localized within the pump volume, and the reduced heat capacity of diamond at cryogenic temperatures results in stronger thermal lensing than at room temperature for a given heat load [53]. An additional increase in power handling is uniquely available in diamond due to the ability to enhance the isotopic purity of the material. The combination of reduced ^{13}C concentration to 0.001% and cryogenic operation leads to an overall 1000× increase in thermal conductivity (see also Fig. 3).

The LIDT of coated crystal facets typically limits the pulse energy (for nanosecond-pulsed lasers) and average power obtainable from a laser crystal. However, the LIDT for coatings is highly dependent on coating design and quality, and values are scarcely published. LIDT measurements for uncoated surfaces provide an upper bound, and for 1 ns pulses at a beam radius of 50 μm reported values are 2 GW/cm^2 at 532 nm, 8 GW/cm^2 at 1064 nm, and 20 GW/cm^2 at 10.6 μm [63]. In the CW regime, our own experiments with anti-reflection coated $\{110\}$ diamond facets have shown that they can withstand linear power densities [64] of approximately 4 MW/cm at 1240 nm [65], aided substantially by their direct thermal contact with the high thermal-conductivity substrate.

Kerr self-focusing may determine the ultimate limit for power-scaling of diamond Raman lasers (DRLs). The Kerr nonlinearity in diamond at infrared wavelengths ($n_2 = 4.2 \times 10^{-20}$ m^2/W [57]) is comparable to other optical crystals. The critical power for self-focusing [66] is approximately 1.6 MW for linearly polarized light at 1064 nm.

Other material properties that are known to affect DRL performance include stress birefringence and absorption from impurities (such as nitrogen). Although diamond is nominally an isotropic crystal, in-grown defects give rise to internal stresses that result in substantial birefringence ($\Delta n > 10^{-4}$ [67]). Quality of synthetic diamond has improved over the last decade [68], [69] and CVD-grown samples with uniform low birefringence of $\Delta n < 10^{-5}$ are now readily available. The effects of birefringence on DRLs with high-finesse cavities have been analyzed in detail [70], and include perturbations to the Stokes polarization and gain reduction. However, these effects are diminished for oscillators with output coupling above approximately 10% provided that $\Delta n \leq 10^{-5}$. Parasitic loss in CVD diamond is dominated by absorption due to defects and nitrogen impurities. A nitrogen content of approximately 20 ppb in optical-grade CVD samples gives rise to absorption of approximately 10^{-3} cm^{-1} at 1 μm, and 10^{-2} cm^{-1} at 0.5 μm [68].

III. High Power Oscillators

The earliest efforts to increase the average output power of DRLs included nanosecond-pulse pumped external-cavity lasers [44], [53], [71], synchronously-pumped mode-locked lasers [19], and an intracavity CW laser [72]. An output power of approximately 25 W was reported in 2011 [53], already at a level notably higher than the maximum obtained using any other Raman crystal. Furthermore, the negative impacts of crystal heating on conversion efficiency and beam quality typically observed in other crystals when overpowered (see eg., [73]) were not observed. Since then, almost all power scaling has been performed in the CW regime using an external-cavity configuration.

A. CW and Quasi-CW External Cavity DRLs

The external-cavity configuration, resonant at only Stokes wavelengths, has several important advantages for investigating high power operation. Firstly, it enables DRLs to act as downstream converters to a wide variety of pump lasers. External cavity designs are readily applicable to pumps operating over a range of wavelengths, such as Ti:sapphire lasers at 800–1000 nm [74], frequency-doubled, tripled or quadrupled Nd^{3+} or Yb^{3+} lasers at 532 nm, 355 nm and 266 nm [15], [23], [52], optical parametric oscillators in the mid-infrared [24], and high-power fiber amplifiers [75]. Unlike designs that are also resonant at the pump wavelength [35], there is no requirement for SLM inputs. In contrast to intracavity Raman lasers, there is no interplay between spectral, spatial [76] and thermal [16] effects occurring in the pump and Raman media thus greatly simplifying the dynamics and analysis. The design constraints on mirror and crystal coatings are also relaxed compared to intracavity designs as the loss requirements at the pump wavelength are not as stringent.

The first external-cavity CW DRL was reported in 2012, achieving 10 W pump-limited output power with 32% conversion efficiency [77] by using tight focusing into the diamond (radius $w_\mathrm{p} = 30\,\mu$m) and 0.4% output coupling. The diamond and its anti-reflection coatings withstood intracavity powers of over 5 kW and intensities on the order of 180 MW/cm^2. The output beam was diffraction-limited despite more than 11 W of heat deposited in the small focal volume (power density $>4 \times 10^5$ W/cm^3). This result was highly significant in the context of Raman lasers as it paved the way for efficient and high-power Raman conversion of CW beams.

In order to investigate higher powers, we found it convenient to use long-pulse, quasi-CW pumps. For the mode-sizes of

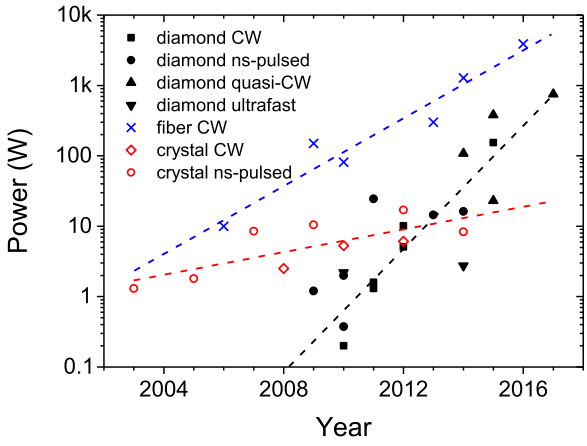

Fig. 4. Achieved average/CW output power of DRLs [15], [17]–[21], [44], [53], [65], [71], [72], [75], [77], [79]–[82] compared to non-diamond Raman crystals [72], [73], [83]–[89] and Raman fiber lasers [90]–[95]. On-time powers are used for quasi-CW (long-pulse) DRLs in the regime of steady-state thermal gradients ($>100\,\mu$s).

interest ($<100\,\mu$m), thermal gradients in diamond establish within a few microseconds [65] so that for longer times the behavior represents thermal steady-state operation under the assumption that the crystal faces are maintained at a fixed temperature. As a result, pumps of duration as short as a few tens of microseconds can be used to investigate CW power scaling behavior. This approach was used to demonstrate a 100 W DRL that was pumped using 0.2 ms-long pulses from a Nd:YAG laser. The output power was pump-limited, with no signs of thermal roll-off or beam quality degradation.

Higher powers and longer on-time durations were achieved by pumping with kW-class seeded-fiber amplifiers in collaboration with the group of Dr. T. Schreiber at the Fraunhofer IOF in Jena. The output linewidth was in the range 40–55 GHz [78] which was sufficiently narrow to achieve high gain and modest thresholds. CW output powers up to 154 W were obtained for durations of 5 s, limited by pump beam delivery components and isolation of the back-reflected pump power. Pumping for 10 ms durations enabled this limit to be extended and yielded up to 380 W output power at 61% conversion efficiency [75]. In both cases, no thermal roll-over or saturation was observed. Most recently, we have used a long-pulse Nd:YAG pump providing 1700 W for durations longer than 0.25 ms to obtain 750 W output power, again without saturation. These results foreshadow excellent prospects for further power scaling of DRLs to the 1 kW level and beyond, with the available option of increasing beam sizes in the diamond to avoid thermal or optical nonlinearities at elevated powers.

Tracking of the steady-state average power (CW, quasi-CW or pulsed) over the last 10 years (Fig. 4) shows that power capability has increased by approximately an order of magnitude every 2–3 years. The highest powers are currently 2–3 orders higher than any other Raman crystal and, we believe, are higher than for any other end-pumped bulk-crystal oscillator (Raman or inversion) operating at room temperature. The highest power Raman lasers are those based on Raman fibers operating near 1.1 μm (eg., 3.89 kW at 1123 nm [94]). Future increases in DRL power are likely with improved availability of suitable pumps and subject to the thermal limits as discussed in the following section.

B. Thermal Analysis

Using finite element modeling (LasCAD), we have estimated the on-axis temperature rise in diamond under first-Stokes lasing with 1 kW pump power at 1064 nm, while maintaining only the bottom crystal face at room temperature. Assuming double-pass pumping with 82% pump depletion (approximated in the software by a pump absorption coefficient of 0.106 mm^{-1}), the quantum defect gives rise to a heat load of 116 W. For a 100 μm radius pump beam, for example, the calculated on-axis temperature rise is 4.3 °C. To contrast this with more familiar end-pumped laser materials, it is worthwhile considering the equivalent temperature rise for the high-power laser crystal Nd:YAG. Using the same pump spot size and double-ended pumping (with evenly-split pump power), only 1.5 W of pump power (and a heat load of 0.42 W) is required to generate an equivalent on-axis temperature rise in the Nd:YAG of 4.3 °C. For a heat load of 114 W, the projected temperature rise would be above 1100 °C and easily above the threshold for stress fracture (22 W for a 1.1 at.% doped Nd:YAG laser [56]).

Even though the extreme thermal properties of diamond provide great potential for achieving high output power, we have already attained levels beyond that expected from first-order thermal lens considerations. The on-axis temperature rise calculated based on thermal conduction from the pumped volume surpasses the threshold for substantially perturbing the laser cavity stability via the thermo-optic mechanism. For the example of the 380 W DRL in [75], we calculated that the thermo-optic lens strength would be at least 83 diopters, which is higher than the predicted value for severe beam degradation and power roll-off ($\sim$30 diopters). As noted in Section II-B, we expect birefringence and end-face distortion effects to be minor on account of diamond's low thermal expansion coefficient. The lack of observed power rollover or beam degradation highlights the need to improve our current understanding of power deposition and heat transport in the diamond.

Reconciliation of this problem is a topic of our current study. One possibility is that the heat is deposited in a larger volume than assumed. Our current model of localized heat deposition is based on the short diffusion lengths of Raman-generated optical phonons. Given the small wavevector of the optical phonons, their propagation distance is negligible before they decay on the timescale of 10^{-10} s [96]. However, the details of the decay products will require consideration. Decay occurs via creation of acoustic phonons [97], [98], but branching ratios to two-three- and four-phonon decay, and the propagation distances for phonons of corresponding energy, are not well known. If propagation distances are significant with respect to the beam radius, this could alleviate the thermal gradients in the diamond. For example, a doubling in radius of the heat deposition zone would reduce the thermal lens strength by a factor of four. This highlights the need for more quantitative measurements of the spatial overlap of pump and Stokes modes, phonon decay and

temperature profiles in order to obtain meaningful predictions of performance at higher power. In the meantime, it is likely that further large increases in the thermally-unaffected power range beyond that of the early modelling predictions will be obtained when using higher power pumps. By comparison with other end-pumped lasers, such as diode-pumped neodymium- or ytterbium-doped YAG lasers, the onset of thermal effects is typically observed well in advance of the maximum achievable output power. Changes in output beam divergence, degradation in beam quality and perturbations to slope efficiency are typical phenomena observed well before the maximum power level set by thermally-induced stress fracture [99], [100]. Indeed, the present diamond laser powers are currently orders of magnitude below the predicted 1 MW stress-fracture limit [101]. Possible power-limiting mechanisms may also include crystal overheating compounded by thermal runaway induced by increasing absorption and thermal resistance as the diamond temperature rises. Nevertheless, powers two times higher than presently achieved may be reasonably expected without major changes in design. Even higher powers are likely to be accessed by using thermal mitigation schemes such as slabs, waveguides, isotopically-pure diamond or diamond at reduced temperatures.

C. Cascaded-Stokes Lasers

An important recent development in CW diamond Raman oscillators is cascaded-Stokes lasing, as it provides greater wavelength reach, for example to the eye-safe atmospheric transmission window around 1.5–1.6 μm directly from Yb^{3+} or Nd^{3+} laser pumps. The only prior report in the literature of a CW, cascaded-Stokes crystal Raman laser operating in an external-cavity geometry was a second-Stokes barium nitrate laser pumped by an argon ion laser operating with a conversion efficiency of less than 1% and an output power of 25 mW [102].

An efficient, high-power (>100 W), second-Stokes DRL was recently reported, along with an analytical model elucidating the characteristics of power transfer in these lasers [103]. A noteworthy aspect of the cavity design was that it used an output coupling much higher than what is typically optimal for first Stokes operation. Our modeling (see Fig. 5(a)) shows this is required for efficient conversion as it enables the build-up of the first Stokes intensity in the cavity to a level that strongly depletes the pump. Lower output-coupling values suppress pump depletion and lead to low efficiency as borne out by our own experiments [103]–[105] and others [102]. Recently, second Stokes (1.49 μm) DRL output powers of more than 300 W have been achieved (see also Section IV-A) using pump powers of 820 W, corresponding to efficiencies approaching those predicted by the model (Fig. 5(b)). Such powers are at the same level as the highest powers obtained in this wavelength range from fiber lasers [93], [106].

The cascaded-Stokes model has been extended to higher Stokes orders [107], as also shown in Fig. 5(a), revealing that output couplings optimize very differently for odd and even Stokes orders; low optimum output coupling (typically less than 10%) for odd orders and much higher output coupling (in the range 50–95%) for even. This alternating behavior can be understood by considering the power transfer amongst Stokes orders in steady-state for the specific case of a non-resonantly-pumped laser. A critical requirement for a laser of any Stokes order is a high intracavity first Stokes intensity to provide efficient power extraction from the pump in a single- or double-pass of the crystal. As noted above for a second-Stokes laser, the high optimum output coupling forestalls conversion to the second Stokes to ensure such a buildup of an intense cavity first-Stokes field. For a third-Stokes laser with high cavity finesse at the second Stokes, an intense third-Stokes field is required to maintain the loss per round-trip for the second-Stokes that, in turn, is needed to ensure sufficient first-Stokes buildup. Hence, a third-Stokes laser has a relatively low optimum output coupling. And so on. Such inductive reasoning indicates the laser optimizes for low and high intracavity intensities for the pump and first Stokes respectively, and these are repeated in alternating fashion across even and odd orders.

This model also highlights a path to efficient CW Stokes generation at wavelengths for which there is intrinsic parasitic loss in the diamond, such as in the three-phonon absorption region at wavelengths between 2.5 and 3.8 μm (refer Section II-B). DRLs operating on an even Stokes order are far less sensitive to losses at the output wavelength than for odd.

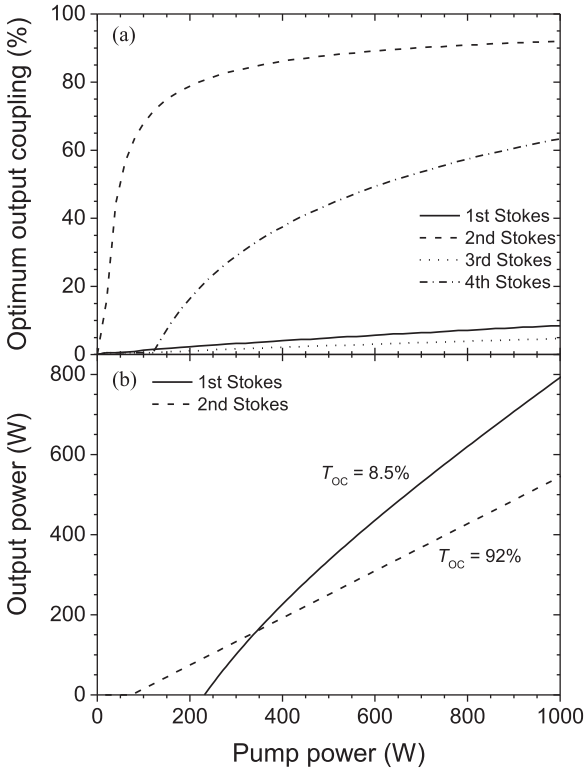

Fig. 5. (a) Optimum output coupling for an nth-Stokes cascaded DRL (n = 1– 4) with a 1064 nm pump focused to a waist radius of 50 μm. For $n > 1$, the cavity is assumed low-loss for all lower-order Stokes lines. The loss at the 4th Stokes wavelength, 2.46 μm, is estimated at 0.3 cm^{-1} (due to multi-phonon absorption), whereas the loss at the shorter wavelengths is taken as 0.0038 cm^{-1}. (b) Modelled output powers for 1st and 2nd Stokes lasers with pump power for output couplings optimized at 1000 W pump power. Note that the 2nd Stokes laser has a lower threshold due to the high cavity finesse at the 1st Stokes wavelength, which gives rise to a highly-enhanced 1st-Stokes intracavity field at lower pump powers.

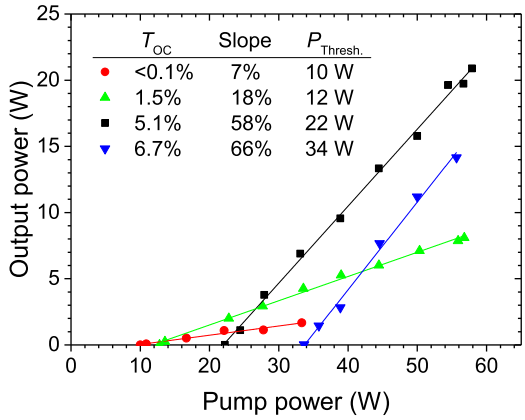

Fig. 6. CW Stokes output power curves at 573 nm for several values of output coupling (T_{OC}), achieved by angle-tuning an intracavity Brewster plate.

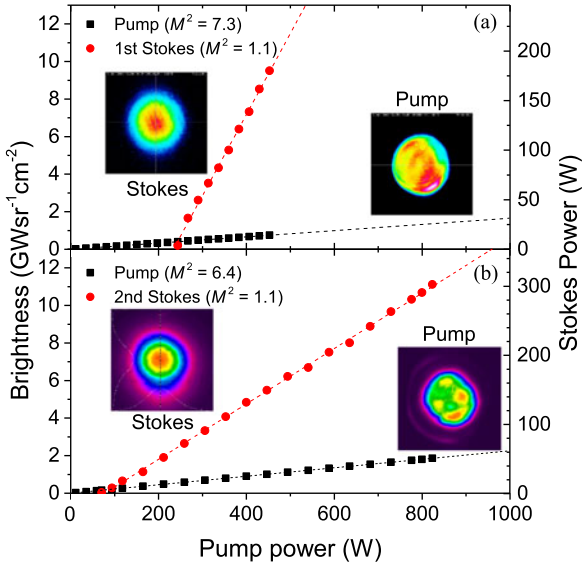

Fig. 7. Brightness of the Stokes output (red circles) and pump input (black squares) as a function of quasi-CW pump power for the (a) first Stokes [113], and (b) second Stokes lasers. Stokes output powers are shown on the right-hand axes. Profiles for the pump and Stokes beams are also shown.

Hence, a second-Stokes DRL pumped at 1.55 μm, for example, may provide an effective route to high power generation near 2.6 μm.

D. Visible Wavelengths

Operation at visible wavelengths is of interest for applications in display, medicine and spectroscopy. We have performed preliminary investigations using a CW 532 nm pump (from a frequency-doubled ytterbium fiber amplifier) to generate 573 nm output via a single Stokes shift. Since diamond has higher absorption loss at visible wavelengths [68], output coupling optimizes at higher values than in the infrared. However, the resultant increase in threshold is offset by the smaller waist radius at focus, and the higher gain coefficient [38] of the shorter-wavelength radiation. Fig. 6 shows power characteristics for several output coupling values via angle adjustment of an intracavity Brewster plate. With single-pass pumping and 58 W pump power, 21 W of 573 nm output was achieved. We believe this approach is suitable for generating output powers well beyond 100 W. We also anticipate that SLM operation is feasible using the principle outlined in Section VI to achieve the MHz linewidths required for effective laser sodium beacons [108] and other spectroscopic applications.

IV. Brightness Enhancement

A. Brightness Conversion in Oscillators

The results presented thus far have been chiefly performed using input of high beam quality ($M^2 < 1.5$). Adaptation of DRLs to inputs of lower beam quality broadens the range of applicable pumps. It is also a prerequisite for increasing brightness beyond that of other high-power technologies (such as fiber, thin-disk and slab lasers). Raman beam cleanup [72], [109]–[112] yielded a 70% increase in brightness over the input beam for a second-Stokes DRL operating in the nanosecond-pulsed regime [44]. Diamond external-cavity converters also provide an opportunity to enhance the brightness of CW beams.

In a recent investigation, we altered the beam quality of a quasi-CW Nd:YAG laser by changing the thermal load and cavity configuration to obtain M^2 values up to 7.3. A DRL threshold intensity of 2.9 MW/cm^2 (230 W) was obtained for the highest M^2 beam by focusing the pump to a small waist (50 μm) in the diamond. With this arrangement, 1240 nm first-Stokes output at 180 W output power was generated with an $M^2 = 1.1$, corresponding to an output brightness 12.7$\times$ higher than the 1064 nm pump [113]. More recently, with cavity mirrors designed for second-Stokes (1485 nm) operation, 302 W of output power was obtained in a diffraction-limited beam, 6.0$\times$ brighter than the pump of power 823 W and $M^2 = 6.4$. The output power and beam quality values are similar to those obtained by erbium-doped fiber lasers and Raman fiber lasers [93], [106]. Fig. 7 shows the pump and Stokes beam brightness as a function of pump power for the first and second-Stokes lasers. In each case, the output beam quality was better than $M^2 = 1.15$.

In these experiments, output beam quality and slope efficiency (81% and 40% for the first- and second-Stokes lasers, respectively) remained high for the entire range of investigated pump M^2 beam factors provided that the pump beam was focused into the cavity fundamental mode. Under such conditions, the threshold for the first-Stokes laser increases by 30% for an M^2 increase from 2.3 to 7.3 [113]. Gain calculations as a function of pump beam quality supported these observations and predict only minor increases in threshold for pumps of $M^2 = 20$ and beyond [113]. These results not only indicate that CW brightness enhancement in diamond is possible, but that large-scale brightness enhancement can be achieved using very poor beam quality pumps. Extrapolating the model calculations suggests that brightness conversion of narrow-linewidth, high-brightness laser diode pumps to diffraction-limited beams using diamond may soon be within reach.

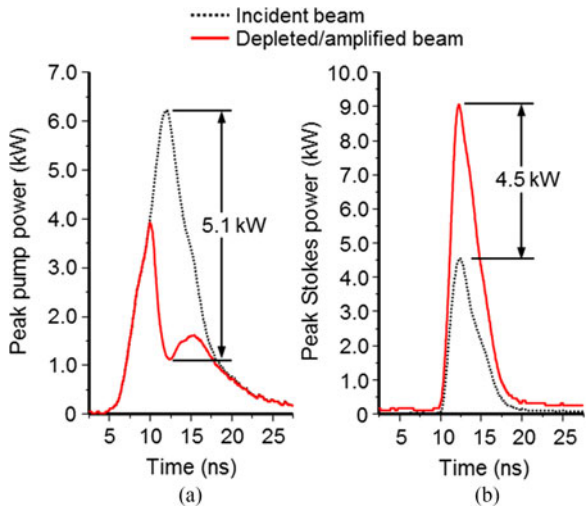

Fig. 8. Temporal pulse profiles for the (a) pump and (b) Stokes seed beams before and after the beam-combining amplifier. The depleted pump energy is efficiently transferred to the Stokes beam.

B. High Power Amplifiers

At higher power levels, it may be advantageous to switch from single Raman oscillators to oscillator-amplifier combinations. We have calculated the minimum Stokes power that would be required to strongly deplete the pump power to realize an efficient power amplifier [114]. Assuming strong focusing of a diffraction-limited pump and Stokes seed to maximize Raman coupling, we find that a seed power of 2 kW is required to deplete 75% of a collinear pump field, decreasing to 0.5 kW for fields refocused back through the amplifier for a second pass. Such Stokes powers are already available from quasi-CW diamond Raman oscillators (Sec III.A) and so efficient CW amplifiers are well within reach.

Once a Stokes beam has been amplified above the kW level, it is feasible to move away from the ideal collinear diffraction-limited beams and use pump lasers with lower beam quality. The Stokes seed power required for efficient extraction scales approximately linearly with the M^2 of the pump beam [79]. We have also studied Raman amplifiers with multiple non-collinear pump beams [45]. The effective beam overlap is reduced for angled beams, so that a higher seed power is required for a given extraction efficiency. For example, three times the seed power is required to efficiently deplete a beam that is laterally displaced by twice its own beam radius on the focusing lens. Non-collinear pumping provides a method for combining multiple input beams simultaneously into a single axial Stokes field. Because each pump beam independently drives a class of phonons with different *k*-vectors and phase, there is no requirement for the pump beams to be mutually coherent.

We have experimentally demonstrated a single-pass Raman amplifier using multiple incoherent pump beams [45]. Using three pump beams with a combined peak power of 6.1 kW, the pump power was depleted by 82% at the pulse peak, as shown in Fig. 8. That depleted power was entirely transferred to an amplified 4.5 kW Stokes seed beam, after allowing for the power loss to the Raman-generated phonons. This experiment used nanosecond, sub-millijoule, pump and Stokes seed pulses at 1 kHz and hence comprises a proof-of-principle for high power beam combination. Provided that single diamond elements are capable of handling continuous powers above the kilowatt level (refer Section III-B), beam combination may be a promising method for scaling laser brightness.

C. High Brightness Nanosecond-Pulsed Systems

The average power handling advantages of diamond also translate to pulsed systems, particularly for systems generating at high duty cycle. For low duty cycles, such as in nanosecond pulsed lasers in which the peak power is much higher than the average power, the limits are determined by the heat capacity of the diamond and factors such as surface damage. The latter is a critical factor and enlarged beam areas are needed to ensure that damage thresholds are not exceeded. This problem is heightened in Raman lasers as the pump and Stokes fields are typically at similarly high levels and combine additively to the stress on elements. Also, for the typical gains required, at least one of the fields has an intensity nearing the damage threshold so that reliability is vulnerable to pulse-to-pulse fluctuations, spikes and beam hot-spots.

A regime of practical interest is high-brightness pulsed output of duration ten- to tens-of nanoseconds for tracking and ranging applications. At the extreme end, pulse energies above 10 mJ are required at tens of kilohertz pulse rates, corresponding to average powers well above 100 W [115]. Such parameters are challenging, even for mature (1 μm) laser materials, due to degradation of beam quality at the high average power [116], [117]. In the case of diamond, its excellent thermal properties are well suited to the high average power loads; however, the rapid heat deposition during the Stokes pulse generation [53], [118] and nonlinear self-focusing (see below) become important design considerations.

We have investigated conversion for a pump pulse duration of 12 ns and energies up to 41 mJ. By increasing the pump spot size to nearly fill the 2 × 2 mm diamond aperture ($w_p = 800\,\mu$m), a threshold of 19.7 mJ was obtained and slope efficiency of 46% (Fig. 9). In these low pulse rate (5 Hz) experiments, the cavity was formed by a flat input coupler and the flat uncoated surface of the diamond as the output coupler ($R = 17\%$). Although the flat-flat cavity is bordering on unstable, it is expected that positive lensing from one or more of gain-guiding, thermal and Kerr effects enables formation of a laser mode. The maximum output energy of 9.7 mJ was produced in a pulse of duration 8 ns and having peak power 1.2 MW. These output energies represent a large increase over previously reported nanosecond-pumped DRLs [44], [71], [118], [119]. The calculated aggregate of pump and Stokes intensity on the crystal facets was 2 J/cm^2, below the expected damage threshold of approximately 10 J/cm^2 [101].

It is interesting to consider the scope for higher energy and peak power. Though the output energy increased linearly with the input, it was noted that the output beam divergence decreased over the same range (for fixed spatial parameters of the input beam) suggesting a nonlinear or thermal effect in the diamond. In the report of [118], a rollover at pulse energies above 1 mJ

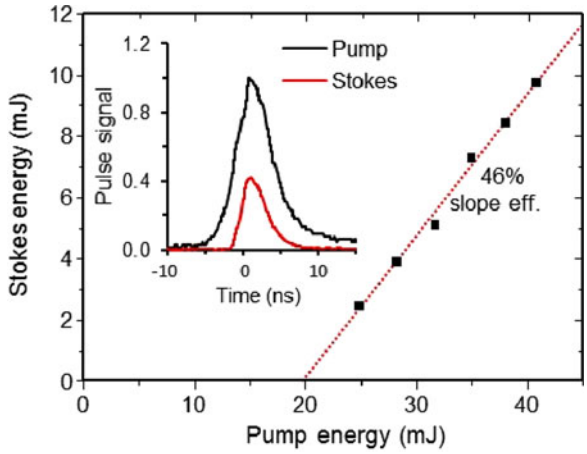

Fig. 9. Energy characteristic for a DRL pumped using large mode area ($w_p = 800\,\mu$m) pump beam. The inset shows the temporal pulse shapes.

(20 ns pulses) was attributed to thermo-optic lensing induced by the heating from Raman-excited phonon decay. The instantaneous power (>1 MW) and gain ($\sim 10\,\text{cm}^{-1}$) are sufficiently high that Kerr focusing and gain guiding also warrant consideration. Our preliminary analysis of the system of Fig. 9 suggests that the observed reduction in beam divergence at high energy is in poor agreement with a model including thermal lensing alone. It is concluded that a more detailed investigation of spatial dynamics is required to determine suitable models for better predicting the behavior at such high peak powers.

V. Intracavity Frequency Conversion

Wavelength diversity is greatly increased when combining diamond with $\chi^{(2)}$ nonlinear frequency mixing. In intracavity Raman lasers, such frequency mixing has been used to generate CW powers up to 5 W in the yellow and orange spectral region [85], [120], [121]. Adaptation to CW external-cavity Raman lasers also provides an important method to generate shorter wavelengths while preserving the practical advantages noted in Section III-A in the context of high power external-cavity oscillators. External cavities with harmonic generation have been investigated for pulsed Raman lasers (eg., using tungstate Raman crystals [122], [123]), but not so far for CW devices due to the lack of Raman materials that are capable of handling the average power requirements.

As a first example, we have demonstrated a quasi-CW external-cavity DRL at 620 nm by including a lithium triborate (LBO) crystal into the quasi-concentric linear cavity [124]. The output wavelength in the red spectrum is of interest in laser display applications, medicine and laser spectroscopy.

An LBO crystal ($4 \times 4 \times 10$ mm) cut at $\theta = 85.8^\circ$ and temperature tuned to 311 K was placed on a translation stage adjacent the diamond (Fig. 10(a)) to enable tuning of the Stokes beam size in the LBO and thus the nonlinear output coupling. Pumping was performed for periods of 0.25 ms. Fig. 11 shows the power dependence on the diamond - LBO separation and the calculated Stokes beam radius in the LBO. The SHG power increases initially up to the 30 W maximum at a separation of

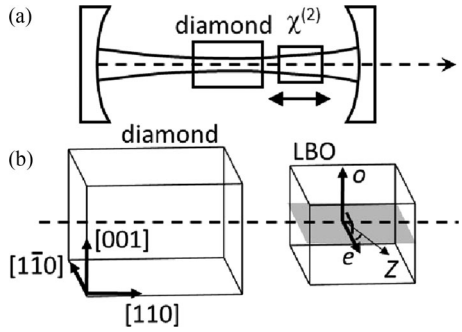

Fig. 10. (a) Experimental arrangement for intracavity harmonic generation. The separation distance between the diamond and harmonic crystals was adjusted to optimize output coupling. (b) The crystal orientations with respect to the propagation axis. The LBO was cut with respect to the optic axis (*Z*) for Type I phase matching. The fundamental (*e*) and Stokes (*o*) polarizations are indicated.

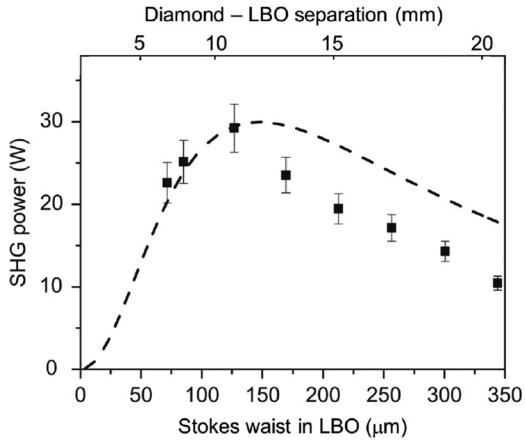

Fig. 11. On-time SHG power as a function of Stokes beam radius in the LBO for 200 W of input power. The dashed line indicates the model calculations of [124].

12 mm (corresponding to a Stokes beam radius in the LBO of 155 μm) and decreases thereafter. For larger than optimum separations, under-coupling occurs in which Stokes-SHG conversion is limited by parasitic loss of the intense intracavity Stokes field. Conversely, over-coupling occurs for smaller than optimum separations which suppresses the Stokes field thus reducing power transfer from the pump and hence maximum obtainable overall conversion efficiency. Modelling [124] based on the formalism in [79] reproduces these regimes of operation (Fig. 11) and agree well with the experimental results.

Although there are several other technologies capable of such powers in this part of the spectrum (diode arrays, VECSELs, Pr lasers, Raman fiber lasers with external-cavity harmonic generation), each of these, except perhaps Raman fibers, have challenges in terms of beam quality at these power levels.

The next natural steps to development are to increase power and extend the on-time duration. Due to the much lower thermal conductivity of LBO, impurity absorption in the LBO becomes a major factor in determining the power limits. Thermal gradients establish much more slowly ($\tau \sim 20$ ms) than in the diamond and over a much longer period than the pump pulse duration; hence the LBO cannot be considered as being in steady-state for

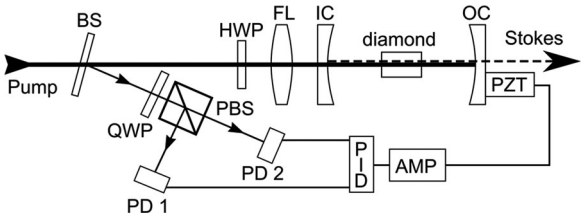

Fig. 12. Active stabilization of cavity length of a near concentric resonator using the Hänsch-Couillaud-type locking scheme. BS beam sampler, FL focusing lens IC input coupler, OC output coupler, PZT piezo actuator, QWP quarter-wave plate, HWP half-wave plate, PBS polarizing beam splitter, PD photodiode, PID controller, AMP high voltage amplifier.

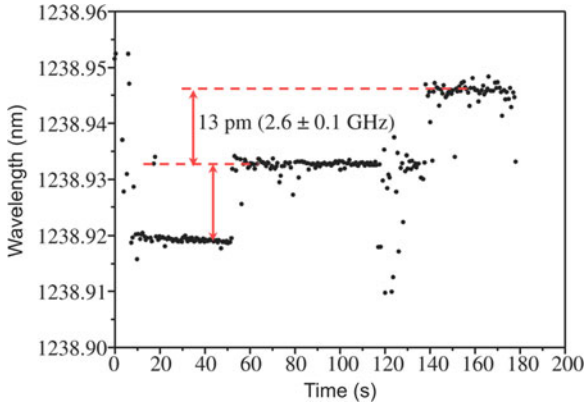

Fig. 13. Wavemeter output (Bristol Instruments) for an actively-stabilized DRL at 4.3 W output power over several minutes of operation. In this case, mode-hopping over two longitudinal cavity modes (FSR = 1.3 GHz) was observed.

these experiments. Nevertheless calculations [124] suggest that, for the present LBO crystal (absorption coefficient 0.1% cm^{-1} at 1064 nm), powers up to 90 W are anticipated before thermal lensing becomes a major factor. Lower impurity LBO is readily available (eg., $<0.05\%$ cm^{-1}) and will aid in power scaling beyond this range.

The concept described here offers the potential to generate other wavelengths in the visible and UV spectral regions by making use of cascaded Stokes orders as well as by using pumps at other wavelengths. Yb-based pump lasers between 1010 nm and 1100 nm, for example, provide a route to wavelengths ranging from 580–640 nm, a range that overlaps wavelengths important for sodium beacons (589 nm) and atom cooling. An important extension of this concept is in the UV where there is demand in spectroscopy, atom cooling and trapping, photolithography, and material processing. One example is a 532 nm-pumped system to generate output at 287 nm wavelength. This would provide a novel alternative route to CW deep UV output with potentially higher power, efficiency and beam quality than current approaches [125]–[129].

VI. High Power SLM Oscillators

As mentioned in Section II, the absence of spatial hole burning in DRLs is beneficial for achieving stable SLM operation. This feature provides an opportunity to more easily generate output with high spectral power densities using simple resonators including standing-wave types.

Investigations were conducted using an external-cavity DRL pumped by a narrow-linewidth (<40 MHz) 1064 nm laser of maximum power 30 W. SLM powers of 4 W and 0.5 W were demonstrated for first- [40] and second- [130] Stokes lasers, respectively. The mode stability of the second-Stokes laser was further improved by using a volume Bragg grating (VBG) mirror in a coupled cavity configuration. However, stability at higher power proved to be difficult due to shifts in Raman resonance with crystal temperature and the interaction between Stokes power and optical cavity length.

In order to compensate for these effects, we have used a Hänsch-Couillaud-type (HC) locking technique to stabilize the near concentric cavity (see Fig. 12). A locking signal was generated from the effects of residual birefringence and the polarization-dependent depletion provided by the Raman conversion. The contribution by the Raman process was found to be essential as cavity locking was stable only above the Raman lasing threshold. The highest SLM output power achieved was 7.2 W for several seconds with the longer-term stability being affected by a combination of cavity drift and a weak locking signal. The stability improved to minutes when lowering the power to 4.3 W although some mode-hopping was also observed (see Fig. 13). As mode instabilities were aggravated with increasing power, more robust stabilization schemes are needed for powers above 5 W. For example, locking schemes based on an auxiliary reference at a wavelength in resonance with the cavity may provide improved stability.

SLM operation has also been investigated for doubly-resonant cavities (ie., resonant for pump and Stokes wavelengths) which enabled thresholds to be reduced to approximately 1 W. Using a ring cavity configuration, 1 W of SLM power has been demonstrated from 5 W pump power from a Ti:sapphire laser [74]. When the intracavity Stokes field propagated in both directions occasional mode instabilities occurred. However, unidirectional operation and stable SLM output was readily achieved using either a retro-reflecting mirror or intracavity sum frequency mixing. These results foreshadow an effective alternative approach to optical parametric oscillators/amplifiers for frequency shifting of multi-watt SLM lasers.

Future work is aimed towards improving the power and frequency stability of SLM operation in both singly- and doubly-resonant cavity configurations. For higher-power output, stable SLM output may be best achieved using master-oscillator power-amplifier configurations. It is interesting to note that, due to the finite Raman gain bandwidth, amplifiers pumped by multi-longitudinal- and multi-transverse-mode pump beams, and by multiple non-collinear beams [45], are expected to still enable efficient power transfer onto a spectrally narrowed and diffraction-limited seed beam.

VII. Conclusions and Future Outlook

The preceding Sections describe five distinct directions of high power DRL development - high power CW lasers with and without intracavity harmonic generation, pulsed nanosecond lasers, SLM lasers and beam combining amplifiers. Ultrafast

lasers, though not yet demonstrated at powers above a few watts [19], are also a potential area for high average power development. The available wavelength range for Raman lasing and amplification is extraordinary compared to most other laser technologies due to diamond's large transmission window. Hence, DRLs and amplifiers comprise a generic laser technology of broad application and with outstanding potential for extending the power and brightness range of lasers, and simultaneously offering additional wavelength choice. The thermal advantages of diamond have been exploited to demonstrate high steady-state powers (>100 W) from extremely small active volumes ($w_s \sim 50\,\mu$m; $l = 5 - 10$ mm) highlighting the capacity for operation at extreme power densities ($>1.5\,\mathrm{MW/cm^3}$) [75]. In the CW or long pulse regimes, the technology benefits from an exceptionally high damage threshold for the anti-reflection coatings ($>200\,\mathrm{MW/cm^2}$).

The distinctive properties of the Raman gain mechanism in combination with those of the diamond material itself present large opportunities as well as some challenges. Compared to other Raman crystals, the characteristically large Raman shift, pure first-order Raman spectrum and the massively improved thermal properties, are facilitating a stepwise jump in Raman laser capability. To date, this has been most evident in high average power conversion of nanosecond pulses [53], the efficient CW conversion in an external cavity [77] (in contrast to crystals with more complex Raman spectra [104]) and quasi-CW laser powers of 750 W (refer Section III-A). The particular symmetry of the diamond lattice also provides a means to efficiently convert unpolarized pumps [131].

Compared to inversion lasers, the contrasting gain mechanism dictates that Raman lasers differ substantially in design and capability. The Raman gain medium may be crudely thought of as inherently gain switched, with additional wavelength versatility provided through Stokes cascading and pump wavelength choice, and with typically tighter constraints on pump linewidth (Section II). Such a description, although it neglects some aspects such as transient behavior ($\tau < T_2$) and some details of beam cleanup and four wave mixing, explains a large fraction of the phenomenology observed. Raman lasers have often been perceived, at least in the past, as a nonlinear conversion technique for wavelength-shifting a given pump laser with a simultaneous benefit to beam quality often obtained through Raman beam cleanup. The demonstrated ability for diamond to be pumped by low spatial coherence beams or multiple beams (refer Section V), suggests a Raman laser technology that is more akin to more familiar optically-pumped inversion lasers. Indeed, we anticipate that direct diode pumping of free-space (unguided) diamond lasers is feasible in the next few years as the spectral and spatial brightness of diode pumps continues to increase. Such direct diode pumping would represent a major advance for high brightness beam generation as well as a notable simplification of systems. The absence of spatial hole burning in the Raman medium has implications for the output spectrum and provides a simplified approach for realizing multi-watt SLM lasers.

These distinctive aspects of the technology provide important opportunities for addressing the needs of applications. Many of these areas have been mentioned previously in the above

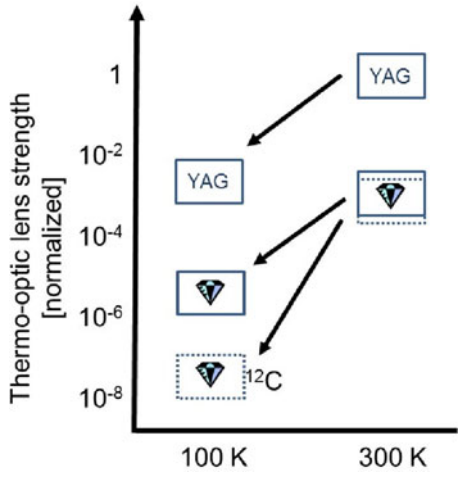

Fig. 14. The relative thermo-optic lens strength ($\mathrm{d}n/\mathrm{d}T/\kappa$) in YAG and diamond showing the scale of enhancements available at reduced temperature and for isotopically-enriched (99.999% ^{12}C) material.

Sections, and include: the generation of high power 1.2 μm and 1.5 μm lasers for applications in remote sensing, tracking and ranging and directed energy; extension of the tuning range of Ti:sapphire lasers; high brightness and high spectral power density lasers in the red-yellow region for spectroscopic applications, sodium guide stars and atom cooling; high power 2–3 μm lasers for materials processing of polymers. These are just a few of the many possibilities. Our own research has been steered by some of these applications; however, the greater vision for DRLs will only be realized once the limits of the technology (wavelength, linewidth, pulse duration, power) are better understood. In terms of power, there are currently major uncertainties in the mechanisms that will come into play as powers increase and ultimately determine the maximum power or power per diamond element in a laser chain. A primary aspect of uncertainty concerns the thermally-induced limits for diamond at room temperature. Currently, no clear signs of beam degradation or power roll-off have been observed and efficient high brightness output was obtained at beam powers more than 2 times higher than expected (refer Section III.B). A possible discrepancy is also evident in our work in the nanosecond-pulsed regime (Section IV-C), although it should be noted that thermal effects have been used to explain rollover in one investigation by others [118]. While these outcomes indicate that improved knowledge of heat deposition and transfer in diamond is required, it also highlights an opportunity for operating in regimes more extreme than originally envisaged. Looking further ahead, massively extended thermal enhancements (by 2–3 orders of magnitude) appear to be accessible through lowering diamond temperature and using diamond of higher isotopic purity (refer Section II-B). Such an isotopic benefit is only accessible for undoped materials, and is much more practical to synthesize for a single elemental material. Hence, diamond provides a unique opportunity to explore extreme regimes of power density in laser physics. The diagram in Fig. 14 compares the thermo-optic lens susceptibility, here defined to scale as $(\mathrm{d}n/\mathrm{d}T)/\kappa$, for diamond and YAG and shows the large reduction available by lowering temperature and for diamond synthesized with low levels of

^{13}C impurity. Analysis suggests that the thermo-optic lens is likely to be more significant compared to stress-fracture, stress-induced birefringence, and crystal distortion, except at powers approaching the megawatt level when Kerr nonlinear focusing effects are expected [45]. Under the assumption that the waste heat can be adequately removed from the crystal surface (ie., with fixed surface temperature), the result would be that continuous average powers above 10^5 W may be generated from a single diamond element of dimensions like those used in the current studies.

Note that such arguments are qualitative and comprehensive numerical models that incorporate an improved understanding of heat dissipation are vital for obtaining more meaningful predictions. It should also be noted that thermal management of such elements will require heat flow from a core crystal to coolants or heatsinks of lower bulk conductivity. Thus, unconventional approaches to thermal engineering are likely to be needed. It is possible that the ultimate limit to power per crystal is not determined by the bulk properties but by the capacity to transfer heat across the boundary.

ACKNOWLEDGMENT

The authors would like to thank D.W. Coutts, H. M. Pask, and M. Dubinskii for stimulating discussions in the course of this work.

REFERENCES

[1] R. Nuttall and A. Frank, "Makers of jewel lenses in Scotland in the early nineteenth century," *Ann. Sci.*, vol. 30, no. 4, pp. 407–416, 1973.
[2] R. W. Ditchburn, "Diamond as an optical material for space optics," *J. Modern Opt.*, vol. 29, no. 4, pp. 355–359, 1982.
[3] C. A. Klein, "Diamond windows for IR applications in adverse environments," *Diamond Related Mater.*, vol. 2, no. 5/7, pp. 1024–1032, 1993.
[4] K. D. Jamison and H. K. Schmidt, "Doped diamond laser," U.S. Patent 5504 767, 1996.
[5] J. P. Goss, P. R. Briddon, M. J. Rayson, S. J. Sque, and R. Jones, "Vacancy-impurity complexes and limitations for implantation doping of diamond," *Phys. Rev. B*, vol. 72, no. 3, 2005, Art. no. 035214.
[6] A. Zunger, "Practical doping principles," *Appl. Phys. Lett.*, vol. 83, no. 1, pp. 57–59, 2003.
[7] G. Eckhardt, D. Bortfeld, and M. Geller, "Stimulated emission of Stokes and anti-Stokes Raman lines from diamond, calcite, and α-sulfur single crystals," *Appl. Phys. Lett.*, vol. 3, pp. 137–138, 1963.
[8] G. Eckhardt, "Selection of Raman laser materials," *IEEE J. Quantum Electron.*, vol. QE-2, no. 1, pp. 1–8, Jan. 1966.
[9] A. K. McQuillan, W. R. L. Clements, and B. P. Stoicheff, "Stimulated Raman emission in diamond: Spectrum, gain, and angular distribution of intensity," *Phys. Rev. A*, vol. 1, pp. 628–635, 1970.
[10] M. Levenson, C. Flytzanis, and N. Bloembergen, "Interference of resonant and nonresonant three-wave mixing in diamond," *Phys. Rev. B*, vol. 6, 1972, Art. no. 3962.
[11] M. Levenson and N. Bloembergen, "Dispersion of the nonlinear optical susceptibility tensor in centrosymmetric media," *Phys. Rev. B*, vol. 10, 1974, Art. no. 4447.
[12] N. Lawandy and R. Afzal, "Solid state diamond Raman laser," U.S. Patent 20050163169 A1, 2004.
[13] A. A. Kaminskii, V. G. Ralchenko, V. I. Konov, and H. J. Eichler, "High-order Stokes and anti-Stokes Raman generation in CVD diamond," *Phys. Status Solidi (B)*, vol. 242, pp. R4–R6, 2005.
[14] A. A. Kaminskii *et al.*, "High-order stimulated Raman scattering in CVD single crystal diamond," *Laser Phys. Lett.*, vol. 4, pp. 350–353, 2007.
[15] R. P. Mildren, J. E. Butler, and J. R. Rabeau, "CVD-diamond external cavity Raman laser at 573 nm," *Opt. Express*, vol. 16, pp. 18950–18955, 2008.
[16] J. A. Piper and H. M. Pask, "Crystalline Raman lasers," *IEEE J. Sel. Top. Quantum Electron.*, vol. 13, no. 3, pp. 692–704, May/Jun. 2007.
[17] W. Lubeigt *et al.*, "An intra-cavity Raman laser using synthetic single-crystal diamond," *Opt. Express*, vol. 18, pp. 16765–16770, 2010.
[18] W. Lubeigt *et al.*, "Continuous-wave diamond Raman laser," *Opt. Lett.*, vol. 35, pp. 2994–2996, 2010.
[19] D. J. Spence, E. Granados, and R. P. Mildren, "Mode-locked picosecond diamond Raman laser," *Opt. Lett.*, vol. 35, no. 4, pp. 556–558, 2010.
[20] R. P. Mildren and A. Sabella, "Highly efficient diamond Raman laser," *Opt. Lett.*, vol. 34, pp. 2811–2813, 2009.
[21] A. Sabella, J. A. Piper, and R. P. Mildren, "1240 nm diamond Raman laser operating near the quantum limit," *Opt. Lett.*, vol. 35, pp. 3874–3876, 2010.
[22] S. Reilly *et al.*, "Monolithic diamond Raman laser," *Opt. Lett.*, vol. 40, no. 6, pp. 930–933, 2015.
[23] E. Granados, D. J. Spence, and R. P. Mildren, "Deep ultraviolet diamond Raman laser," *Opt. Express*, vol. 19, pp. 20422–20427, 2011.
[24] A. Sabella, J. A. Piper, and R. P. Mildren, "Diamond Raman laser with continuously tunable output from 3.38 to 3.80 μm," *Opt. Lett.*, vol. 39, pp. 4037–4040, 2014.
[25] A. Sabella, "Long wavelength extension of diamond Raman lasers," Ph.D. dissertation, Macquarie Univ., Sydney, Australia, 2017.
[26] P. Latawiec *et al.*, "On-chip diamond Raman laser," *Optica*, vol. 2, no. 11, pp. 924–928, 2015.
[27] P. Latawiec, V. Venkataraman, A. Shams-Ansari, M. Markham, and M. Lončar, "Integrated diamond Raman laser pumped in the near-visible," *Opt. Lett.*, vol. 43, no. 2, pp. 318–321, 2018.
[28] R. W. Hellwarth, "Theory of stimulated Raman scattering," *Phys. Rev.*, vol. 130, no. 5, pp. 1850–1963, 1963.
[29] Y. R. Shen and N. Bloembergen, "Theory of stimulated Brillouin and Raman scattering," *Phys. Rev.*, vol. 137, pp. 1787–1805, 1965.
[30] A. Z. Grasyuk, "Raman lasers," *Sov. J. Quantum Electron.*, vol. 4, no. 3, pp. 269–282, 1974.
[31] A. Penzkofer, A. Laubereau, and W. Kaiser, "High intensity Raman interactions," *Progress Quantum Electron.*, vol. 6, pp. 55–140, 1978.
[32] M. Raymer, J. Mostowski, and J. Carlsten, "Theory of stimulated Raman scattering with broad-band lasers," *Phys. Rev. A*, vol. 19, no. 6, 1979, Art. no. 2304.
[33] J. Murray, J. Goldhar, D. Eimerl, and A. Szoke, "Raman pulse compression of excimer lasers for application to laser fusion," *IEEE J. Quantum Electron.*, vol. QE-15, no. 5, pp. 342–368, May 1979.
[34] J. Lin and D. J. Spence, "25.5 fs dissipative soliton diamond Raman laser," *Opt. Lett.*, vol. 41, no. 8, pp. 1861–1864, 2016.
[35] J. K. Brasseur, K. S. Repasky, and J. L. Carlsten, "Continuous-wave Raman laser in H_2," *Opt. Lett.*, vol. 23, no. 5, pp. 367–369, 1998.
[36] A. S. Grabtchikov *et al.*, "Multimode pumped continuous-wave solid-state Raman laser," *Opt. Lett.*, vol. 29, pp. 2524–2526, 2004.
[37] D. J. Spence, "Spectral effects of stimulated Raman scattering in crystals," *Progress Quantum Electron.*, vol. 51, pp. 1–45, 2017.
[38] A. Sabella, D. J. Spence, and R. P. Mildren, "Pump-probe measurements of the Raman gain coefficient in crystals using multi-longitudinal-mode beams," *IEEE J. Quantum Electron.*, vol. 51, no. 12, Dec. 2015, Art. no. 1000108.
[39] W. R. Trutna, Y. K. Park, and R. L. Byer, "The dependence of Raman Gain on pump laser bandwidth," *IEEE J. Quantum Electron.*, vol. QE-15, no. 7, pp. 648–655, Jul. 1979.
[40] O. Lux, S. Sarang, O. Kitzler, D. J. Spence, and R. P. Mildren, "Intrinsically stable high-power single longitudinal mode laser using spatial hole burning free gain," *Optica*, vol. 3, pp. 876–881, 2016.
[41] A. E. Siegman, *Lasers*. Dulles, VA, USA: University Science Books, 1986.
[42] T. Baer, "Large-amplitude fluctuations due to longitudinal mode coupling in diode-pumped intracavity-doubled Nd:YAG lasers," *J. Opt. Soc. Amer. B*, vol. 3, no. 9, pp. 1175–1180, 1986.
[43] R. Chang, R. Lehmberg, M. Duignan, and N. Djeu, "Raman beam cleanup of a severely aberrated pump laser," *IEEE J. Quantum Electron.*, vol. QE-21, no. 5, pp. 477–487, May 1985.
[44] A. McKay, O. Kitzler, and R. P. Mildren, "Simultaneous brightness enhancement and wavelength conversion to the eye-safe region in a high-power diamond Raman laser," *Laser Photon. Rev.*, vol. 8, pp. L37–L41, 2014.

[45] A. McKay, D. J. Spence, D. W. Coutts, and R. P. Mildren, "Diamond-based concept for combining beams at very high average powers," *Laser Photon. Rev.*, vol. 11, no. 3, 2017, Art. no. 1600130.

[46] R. P. Mildren, "Side-pumped crystalline Raman laser," *Opt. Lett.*, vol. 36, pp. 235–237, 2011.

[47] M. Grimsditch, M. Cardona, J. M. Calleja, and F. Meseguer, "Resonance in the Raman scattering of CaF_2, SrF_2, BaF_2 and diamond," *J. Raman Spectrosc.*, vol. 10, pp. 77–81, 1981.

[48] T. T. Basiev, A. A. Sobol, P. G. Zverev, V. V. Osiko, and R. C. Powell, "Comparative spontaneous Raman spectroscopy of crystals for Raman lasers," *Appl. Opt.*, vol. 38, pp. 594–598, 1999.

[49] O. Boyraz, "Silicon Raman laser, amplifier, and wavelength converter," in *Optical Interconnects*. New York, NY, USA: Springer, 2006, pp. 33–51.

[50] A. McKay, D. J. Spence, D. W. Coutts, and R. P. Mildren, "Non-collinear beam combining of kilowatt beams in a diamond Raman amplifier," in *Proc. Adv. Solid State Lasers Conf.*, 2014, Paper ATu5A.1.

[51] V. Savitski *et al.*, "Characterization of single-crystal synthetic diamond for multi-watt continuous-wave Raman lasers," *IEEE J. Quantum Electron.*, vol. 48, no. 3, pp. 328–337, Mar. 2012.

[52] V. G. Savitski, S. Reilly, and A. J. Kemp, "Steady-state Raman gain in diamond as a function of pump wavelength," *IEEE J. Quantum Electron.*, vol. 49, no. 2, pp. 218–223, Feb. 2013.

[53] J.-P. M. Feve, K. E. Shortoff, M. J. Bohn, and J. K. Brasseur, "High average power diamond Raman laser," *Opt. Express*, vol. 19, pp. 913–22, 2011.

[54] R. P. Mildren, "Intrinsic optical properties of diamond," in *Optical Engineering of Diamond*. Weinheim, Germany: Wiley-VCH Verlag GmbH, 2013, pp. 1–34.

[55] W. Koechner, "Thermal lensing in a Nd:YAG laser rod," *Appl. Opt.*, vol. 9, no. 11, pp. 2548–2553, 1970.

[56] S. C. Tidwell, J. F. Seamans, M. S. Bowers, and A. K. Cousins, "Scaling CW diode-end-pumped Nd:YAG lasers to high average powers," *IEEE J. Quantum Electron.*, vol. 28, no. 4, pp. 997–1009, Apr. 1992.

[57] M. Sheik-Bahae *et al.*, "Optical nonlinearities in diamond," *Proc. SPIE*, vol. 2428, pp. 605–609, 1995.

[58] Y. F. Chen, "Design criteria for concentration optimization in scaling diode end-pumped lasers to high powers: Influence of thermal fracture," *IEEE J. Quantum Electron.*, vol. 35, no. 2, pp. 234–239, Feb. 1999.

[59] E. Abraham and J. M. Halley, "Some calculations of temperature profiles in thin films with laser heating," *Appl. Phys. A*, vol. 42, no. 4, pp. 279–285, 1987.

[60] J. R. Olson *et al.*, "Thermal conductivity of diamond between 170 and 1200 K and the isotope effect," *Phys. Rev. B, Condens. Matter*, vol. 47, no. 22, pp. 14850–14856, 1993.

[61] L. Wei, P. K. Kuo, R. L. Thomas, T. R. Anthony, and W. F. Banholzer, "Thermal conductivity of isotopically modified single crystal diamond," *Phys. Rev. Lett.*, vol. 70, no. 24, pp. 3764–3767, 1993.

[62] S. Stoupin and Y. V. Shvyd'Ko, "Ultraprecise studies of the thermal expansion coefficient of diamond using backscattering X-ray diffraction," *Phys. Rev. B, Condens. Matter*, vol. 83, pp. 1–7, 2011.

[63] C. Klein, "Laser-induced damage to diamond: dielectric breakdown and BHG scaling," *Proc. SPIE*, vol. 2428, pp. 517–530, 1995.

[64] R. M. Wood, "Laser induced damage thresholds and laser safety levels. Do the units of measurement matter?," *Opt. Laser Technol.*, vol. 29, no. 8, pp. 517–522, 1998.

[65] R. J. Williams, O. Kitzler, A. McKay, and R. P. Mildren, "Investigating diamond Raman lasers at the 100 W level using quasi-continuous-wave pumping," *Opt. Lett.*, vol. 39, no. 14, pp. 4152–4155, 2014.

[66] R. W. Boyd, "Processes resulting from the Intensity-dependent refractive index," in *Nonlinear Optics,* 3rd ed. Burlington, NJ, USA: Academic, 2008, pp. 329–390.

[67] H. Pinto and R. Jones, "Theory of the birefringence due to dislocations in single crystal CVD diamond," *J. Phys., Condens. Matter*, vol. 21, no. 36, 2009, Art. no. 364220.

[68] I. Friel, S. Geoghegan, D. Twitchen, and G. A. Scarsbrook, "Development of high quality single crystal diamond for novel laser applications," *Proc. SPIE*, vol. 7838, 2010, Art. no. 783819.

[69] I. Friel, "Optical quality diamond grown by chemical vapor deposition," in *Optical Engineering of Diamond*, R. P. Mildren and J. R. Rabeau, Eds. Weinheim, Germany: Wiley-VCH, 2013, pp. 35–69.

[70] H. Jasbeer *et al.*, "Birefringence and piezo-Raman analysis of single crystal CVD diamond and effects on Raman laser performance," *J. Opt. Soc. Amer. B*, vol. 33, pp. B56–B64, 2016.

[71] A. McKay, H. Liu, O. Kitzler, and R. P. Mildren, "An efficient 14.5 W diamond Raman laser at high pulse repetition rate with first (1240 nm) and second (1485 nm) Stokes output," *Laser Phys. Lett.*, vol. 10, 2013, Art. no. 105801.

[72] V. G. Savitski *et al.*, "Characterization of single-crystal synthetic diamond for multi-watt continuous-wave Raman lasers," *IEEE J. Quantum Electron.*, vol. 48, no. 3, pp. 328–337, Mar. 2012.

[73] R. Chulkov *et al.*, "Thermal aberrations and high power frequency conversion in a barium nitrate Raman laser," *Appl. Phys. B*, vol. 106, pp. 867–875, 2012.

[74] O. Kitzler *et al.*, "Single-longitudinal-mode ring diamond Raman laser," *Opt. Lett.*, vol. 42, pp. 1229–1232, 2017.

[75] R. J. Williams *et al.*, "Efficient Raman frequency conversion of high-power fiber lasers in diamond," *Laser Photon. Rev.*, vol. 9, pp. 405–411, 2015.

[76] D. J. Spence, "Spatial and spectral effects in continuous-wave intracavity Raman lasers," *IEEE J. Sel. Topics Quantum Electron.*, vol. 21, no. 1, Jan./Feb. 2015, Art. no. 1400108.

[77] O. Kitzler, A. McKay, and R. P. Mildren, "Continuous-wave wavelength conversion for high-power applications using an external cavity diamond Raman laser," *Opt. Lett.*, vol. 37, pp. 2790–2792, 2012.

[78] F. Beier *et al.*, "Narrow linewidth, single mode 3 kW average power from a directly diode pumped ytterbium-doped low NA fiber amplifier," *Opt. Express*, vol. 24, no. 6, pp. 6011–6020, 2016.

[79] O. Kitzler, A. McKay, D. J. Spence, and R. P. Mildren, "Modelling and optimization of continuous-wave external cavity Raman lasers," *Opt. Express*, vol. 23, 2015, Art. no. 8590.

[80] W. Lubeigt *et al.*, "1.6 W continuous-wave Raman laser using low-loss synthetic diamond," *Opt. Express*, vol. 19, pp. 6938–6944, 2011.

[81] D. C. Parrotta, A. J. Kemp, M. D. Dawson, and J. E. Hastie, "Tunable continuous-wave diamond Raman laser," *Opt. Express*, vol. 19, pp. 24165–24170, 2011.

[82] A. M. Warrier *et al.*, "Highly efficient picosecond diamond Raman laser at 1240 and 1485 nm," *Opt. Express*, vol. 22, pp. 3325–3333, 2014.

[83] X. H. Chen *et al.*, "Diode side-pumped actively Q-switched Nd:YAG/$SrWO_4$ Raman laser with high average output power of over 10 W at 1180 nm," *Laser Phys. Lett.*, vol. 6, pp. 363–366, 2009.

[84] A. J. Lee, H. M. Pask, P. Dekker, and J. A. Piper, "High efficiency, multi-watt CW yellow emission from an intracavity-doubled self-Raman laser using Nd:$GdVO_4$," *Opt. Express*, vol. 16, pp. 21958–21963, 2008.

[85] A. J. Lee, H. M. Pask, D. J. Spence, and J. A. Piper, "Efficient 5.3 W cw laser at 559 nm by intracavity frequency summation of fundamental and first-Stokes wavelengths in a self-Raman Nd:$GdVO_4$ laser," *Opt. Lett.*, vol. 35, no. 5, pp. 682–684, 2010.

[86] S. Li *et al.*, "Diode-side-pumped intracavity frequency-doubled Nd:YAG/$BaWO_4$ Raman laser generating average output power of 3.14 W at 590 nm," *Opt. Lett.*, vol. 32, no. 20, pp. 2951–2953, 2007.

[87] A. McKay, O. Kitzler, and R. P. Mildren, "High power tungstate-crystal Raman laser operating in the strong thermal lensing regime," *Opt. Express*, vol. 22, pp. 707–715, 2014.

[88] R. P. Mildren, H. M. Pask, H. Ogilvy, and J. A. Piper, "Discretely tunable, all-solid-state laser in the green, yellow, and red," *Opt. Lett.*, vol. 30, pp. 1500–1502, 2005.

[89] H. M. Pask, S. Myers, J. A. Piper, J. Richards, and T. McKay, "High average power, all-solid-state external resonator Raman laser," *Opt. Lett.*, vol. 28, pp. 435–437, 2003.

[90] C. A. Codemard *et al.*, "High-power continuous-wave cladding-pumped Raman fiber laser," *Opt. Lett.*, vol. 31, no. 15, pp. 2290–2292, 2006.

[91] Y. Feng, L. R. Taylor, and D. B. Calia, "150 W highly-efficient Raman fiber laser," *Opt. Express*, vol. 17, no. 26, pp. 23678–23683, 2009.

[92] J. W. Nicholson *et al.*, "Raman fiber laser with 81 W output power at 1480 nm," *Opt. Lett.*, vol. 35, no. 18, pp. 3069–3071, 2010.

[93] V. R. Supradeepa and J. W. Nicholson, "Power scaling of high-efficiency 1.5 μm cascaded Raman fiber lasers," *Opt. Lett.*, vol. 38, no. 14, pp. 2538–2541, 2013.

[94] Q. Xiao *et al.*, "Bidirectional pumped high power Raman fiber laser," *Opt. Express*, vol. 24, no. 6, pp. 6758–6768, 2016.

[95] L. Zhang *et al.*, "Kilowatt ytterbium-Raman fiber laser," *Opt. Express*, vol. 22, no. 15, pp. 18483–18489, 2014.

[96] A. Laubereau, D. von der Linde, and W. Kaiser, "Decay time of hot TO phonons in diamond," *Phys. Rev. Lett.*, vol. 27, no. 12, pp. 802–805, 1971.

[97] P. G. Klemens, "Anharmonic decay of optical phonons," *Phys. Rev.*, vol. 148, no. 2, pp. 845–848, 1966.

[98] N. V. Surovtsev and I. N. Kupriyanov, "Temperature dependence of the Raman line width in diamond: Revisited," *J. Raman Spectrosc.*, vol. 46, no. 1, pp. 171–176, 2015.
[99] W. A. Clarkson, "Thermal effects and their mitigation in end-pumped solid-state lasers," *J. Phys. D, Appl. Phys.*, vol. 34, no. 16, 2001, Art. no. 2381.
[100] P. Loiko *et al.*, "Anisotropy of the photo-elastic effect in Nd: $KGd(WO_4)^2$ laser crystals," *Laser Phys. Lett.*, vol. 11, no. 5, 2014, Art. no. 055002.
[101] R. P. Mildren, A. Sabella, O. Kitzler, D. J. Spence, and A. M. Mckay, "Diamond Raman laser design and performance," in Optical Engineering of Diamond. Weinheim, Germany: Wiley-VCH Verlag GmbH, 2013, pp. 239–276.
[102] A. S. Grabtchikov *et al.*, "Continuous-wave solid-state two-Stokes Raman laser," *Quantum Electron.*, vol. 39, no. 7, 2009, Art. no. 624.
[103] R. J. Williams, D. J. Spence, O. Lux, and R. P. Mildren, "High-power continuous-wave Raman frequency conversion from 1.06 μm to 1.49 μm in diamond," *Opt. Express*, vol. 25, no. 2, pp. 749–757, 2017.
[104] S. Sarang *et al.*, "High-gain 87 cm^{-1} Raman line of KYW and its impact on continuous-wave Raman laser operation," *Opt. Express*, vol. 24, no. 19, pp. 21463–21473, 2016.
[105] A. Sabella, J. A. Piper, and R. P. Mildren, "Efficient conversion of a 1.064 μm Nd : YAG laser to the eye-safe region using a diamond Raman laser," *Opt. Express*, vol. 19, pp. 23554–23560, 2011.
[106] Y. Jeong *et al.*, "Erbium:ytterbium codoped large-core fiber laser with 297-W continuous-wave output power," *IEEE J. Sel. Topics Quantum Electron.*, vol. 13, no. 3, pp. 573–579, May/Jun. 2007.
[107] R. J. Williams, D. J. Spence, O. Lux, and R. P. Mildren, "Cascaded continuous-wave Raman frequency conversion in external-cavity diamond lasers," in *Proc. Lasers Electro-Optics Eur. Eur. Quantum Electron. Conf.*, Paper CA_11_3, 2017.
[108] R. Holzlöhner *et al.*, "Optimization of CW sodium laser guide star efficiency," *Astron. Astrophys.*, vol. 510, 2010, Art. no. A20.
[109] Y. Glick, V. Fromzel, J. Zhang, N. Ter-Gabrielyan, and M. Dubinskii, "High-efficiency, 154 W CW, diode-pumped Raman fiber laser with brightness enhancement," *Appl. Opt.*, vol. 56, no. 3, pp. B97–B102, 2017.
[110] J. T. Murray, W. L. Austin, and R. C. Powell, "Intracavity Raman conversion and Raman beam cleanup," *Opt. Mater.*, vol. 11, pp. 353–371, 1999.
[111] J. Reintjes, R. H. Lehmberg, R. S. F. Chang, M. T. Duignan, and G. Calame, "Beam cleanup with stimulated Raman scattering in the intensity-averaging regime," *J. Opt. Soc. Amer. B*, vol. 3, no. 10, pp. 1408–1427, 1986.
[112] E. A. Zlobina *et al.*, "Generating high-quality beam in a multimode LD-pumped all-fiber Raman laser," *Opt. Express*, vol. 25, no. 11, pp. 12581–12587, 2017.
[113] Z. Bai *et al.*, "Large brightness enhancement for continuous wave beams by diamond Raman laser conversion," *Opt. Lett.*, vol. 43, pp. 563–566, 2018.
[114] A. McKay, R. P. Mildren, D. W. Coutts, and D. J. Spence, "SRS in the strong-focusing regime for Raman amplifiers," *Opt. Express*, vol. 23, pp. 15012–15020, 2015.
[115] G. P. Perram, M. A. Marciniak, and M. Goda, "High energy laser weapons: Technology overview," *Proc. SPIE*, vol. 5414, pp. 1–25, 2004.
[116] P. Russbueldt *et al.*, "Innoslab amplifiers," *IEEE J. Sel. Topics Quantum Electron.*, vol. 21, no. 1, Jan./Feb. 2015, Art. no. 3100117.
[117] N. Baranova *et al.*, "Compact sources for eye-safe illumination," *Proc. SPIE*, vol. 10082, 2017, Art. no. 1008209.
[118] V. Pashinin *et al.*, "External-cavity diamond Raman laser performance at 1240 nm and 1485 nm wavelengths with high pulse energy," *Laser Phys. Lett.*, vol. 13, no. 6, 2016, Art. no. 065001.
[119] S. Reilly *et al.*, "Energy scaling of yellow emission from monolithic diamond Raman lasers," in *Proc. Lasers Electro-Opt. Eur. Eur. Quantum Electron. Conf.*, Paper CD_P_22, 2017.
[120] H. M. Pask, P. Dekker, R. P. Mildren, D. J. Spence, and J. A. Piper, "Wavelength-versatile visible and UV sources based on crystalline Raman lasers," *Progress Quantum Electron.*, vol. 32, pp. 121–158, 2008.
[121] D. C. Parrotta, A. J. Kemp, M. D. Dawson, and J. E. Hastie, "Multi-watt, continuous-wave, tunable diamond Raman laser with intracavity frequency-doubling to the visible region," *IEEE J. Sel. Topics Quantum Electron.*, vol. 19, no. 4, Jul./Aug. 2013, Art. no. 1400108.
[122] R. P. Mildren, H. Ogilvy, and J. A. Piper, "Solid-state Raman laser generating discretely tunable ultraviolet between 266 and 320 nm," *Opt. Lett.*, vol. 32, pp. 814–816, 2007.
[123] H. M. Pask, R. P. Mildren, and J. A. Piper, "Optical field dynamics in a wavelength-versatile, all-solid-state intracavity cascaded pulsed Raman laser," *Appl. Phys. B*, vol. 93, no. 2/3, pp. 507–513, 2008.
[124] H. Jasbeer, R. J. Williams, A. McKay, and R. P. Mildren, "Wavelength diversification of high-power external cavity diamond Raman lasers using intracavity harmonic generation," *Opt. Express*, vol. 26, pp. 1930–1941, 2018.
[125] T. Gün, P. Metz, and G. Huber, "Efficient continuous wave deep ultraviolet Pr^{3+} : $LiYF_4$ laser at 261.3 nm," *Appl. Phys. Lett.*, vol. 99, no. 18, 2011, Art. no. 181103.
[126] T. Südmeyer *et al.*, "Efficient 2nd and 4th harmonic generation of a single-frequency, continuous-wave fiber amplifier," *Opt. Express*, vol. 16, no. 3, pp. 1546–1551, 2008.
[127] Y. Kaneda *et al.*, "Continuous-wave all-solid-state 244 nm deep-ultraviolet laser source by fourth-harmonic generation of an optically pumped semiconductor laser using $CsLiB_6O_{10}$ in an external resonator," *Opt. Lett.*, vol. 33, no. 15, pp. 1705–1707, 2008.
[128] M. Scheid *et al.*, "750 mW continuous-wave solid-state deep ultraviolet laser source at the 253.7 nm transition in mercury," *Opt. Lett.*, vol. 32, no. 8, pp. 955–957, 2007.
[129] B. Wellmann, D. J. Spence, and D. W. Coutts, "Tunable continuous-wave deep-ultraviolet laser based on Ce:LiCAF," *Opt. Lett.*, vol. 39, no. 5, pp. 1306–1309, 2014.
[130] O. Lux, S. Sarang, R. J. Williams, A. M. Mckay, and R. P. Mildren, "Single longitudinal mode diamond Raman laser in the eye-safe spectral region for water vapor detection," *Opt. Express*, vol. 24, pp. 876–881, 2016.
[131] A. McKay, A. Sabella, and R. P. Mildren, "Polarization conversion in cubic Raman crystals," *Sci. Rep.*, vol. 7, 2017, Art. no. 41702.

Authors' photographs and biographies not available at the time of publication.